# Additional Data: Original Gel Pics

b

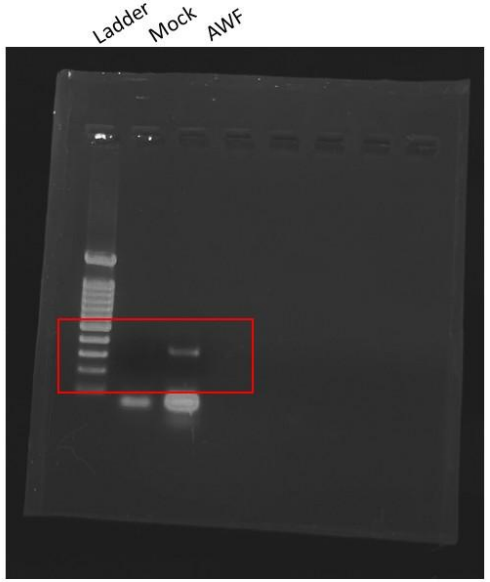


Fig. 2 (b) RT-PCR detection of ASSVd in the ASSVd infected AWF and mock as control.

c

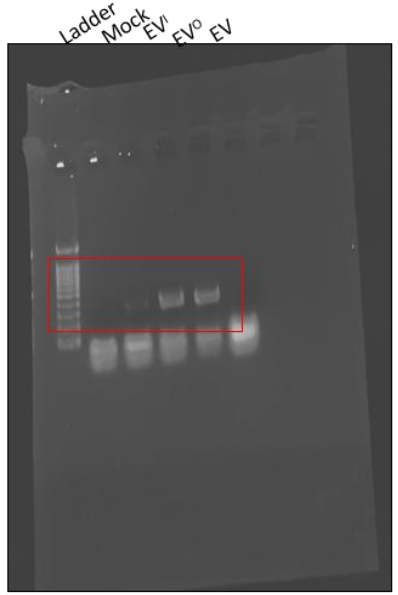


Fig. 2 (c) RT-PCR detection of ASSVd in the total EV fraction obtained via SEC (EV), $EV^{O}$ fraction after trypsin treatment and RNA isolation without EV disruption, and $EV^{I}$ fraction after trypsin, RNase and detergent treatment followed by RNA isolation from inside the EVs.

d

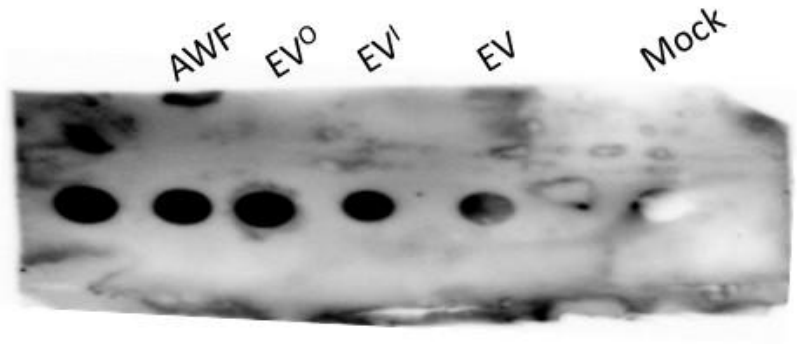


Fig. 2 (d) Dot blot detection of ASSVd in the AWF, total EV fraction obtained via SEC (EV), $EV^{O}$ fraction after trypsin treatment and RNA isolation without EV disruption, and $EV^{I}$ fraction after trypsin, RNase and detergent treatment followed by RNA isolation from inside the EVs

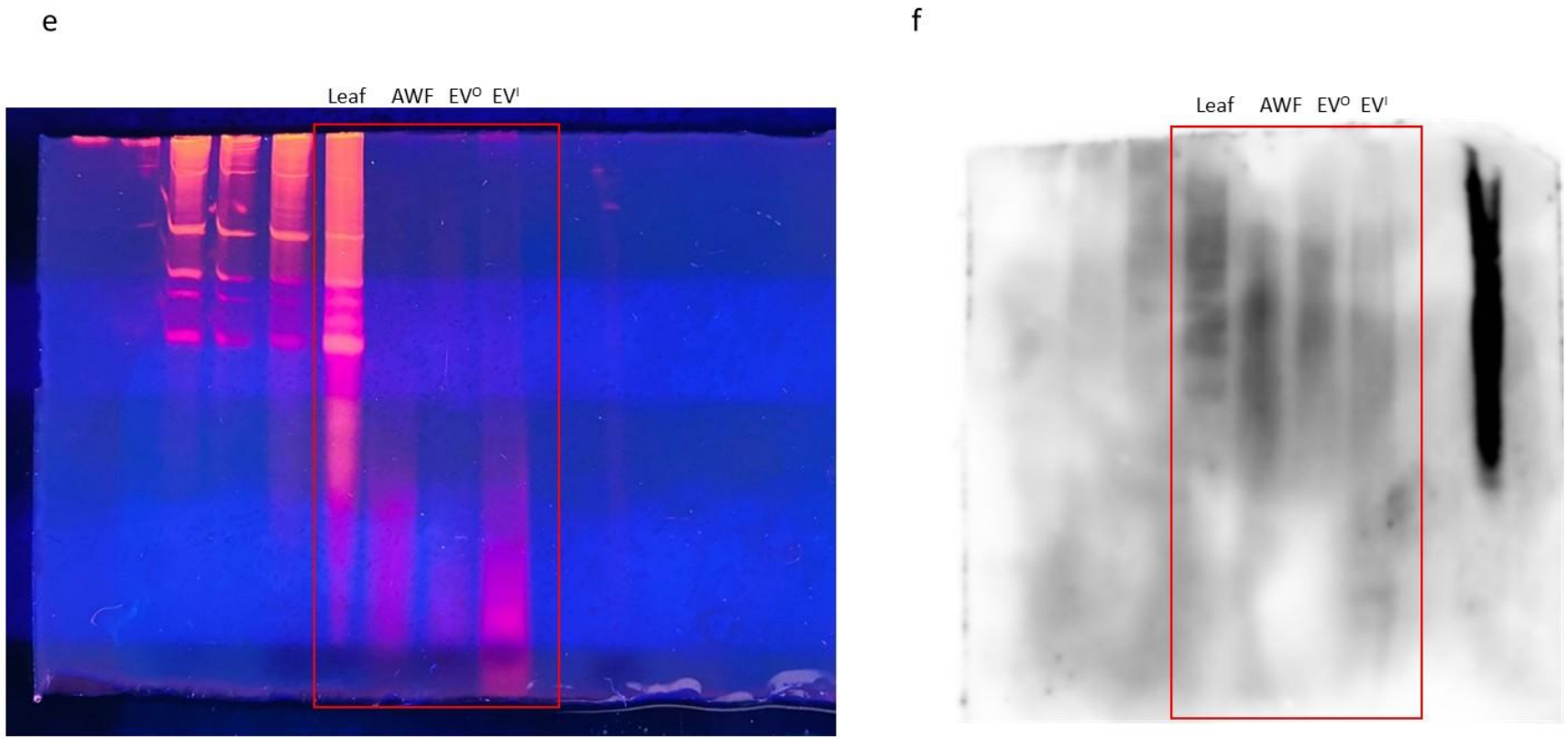


Fig. 2 (e) EtBr-stained gel showing RNA from infected leaves and their corresponding AWF and EV fractions
(f) Northern blot of the same gel using a 3'-labeled biotin-negative sense ASSVd probe, revealing both circular and linear forms of ASSVd in AWF and inside and outside EVs. Small RNAs of ASSVd are distinctly visible within the EV fraction.

(h)

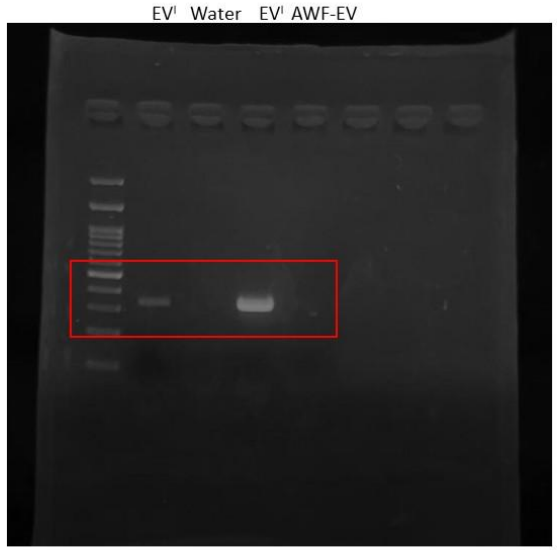


Fig. 2 (h) RT-PCR showing detection of ASSVd in plants fed with whiteflies that were pre-fed on viroid-infected EVs, with water serving as the control.

i


Fig. 2 (i) RT-PCR analysis of cucumber plant sap inoculated with leaf tissue, AWF, and EVs from viroid-infected plants, revealing a 330 bp amplification corresponding to the ASSVd genome using viroid-specific primers. Plants inoculated with water, used as a mock control, did not show the presence of the viroid, serving as a negative control in the assay.

(g)

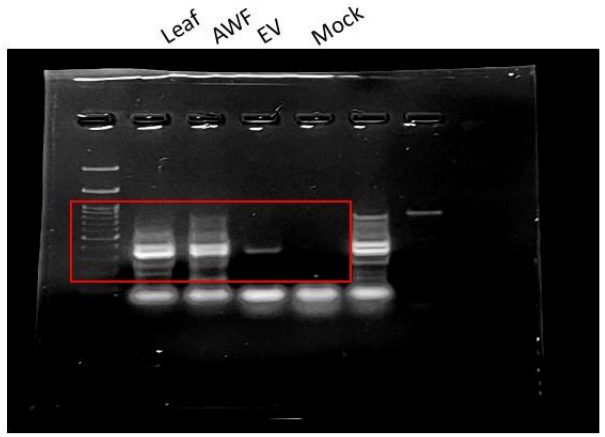


Fig. 2 (g) RT-PCR showing detection of the viroid within EVs, whiteflies fed with intact EVs, apoplast lacking EVs, and water as the mock control.

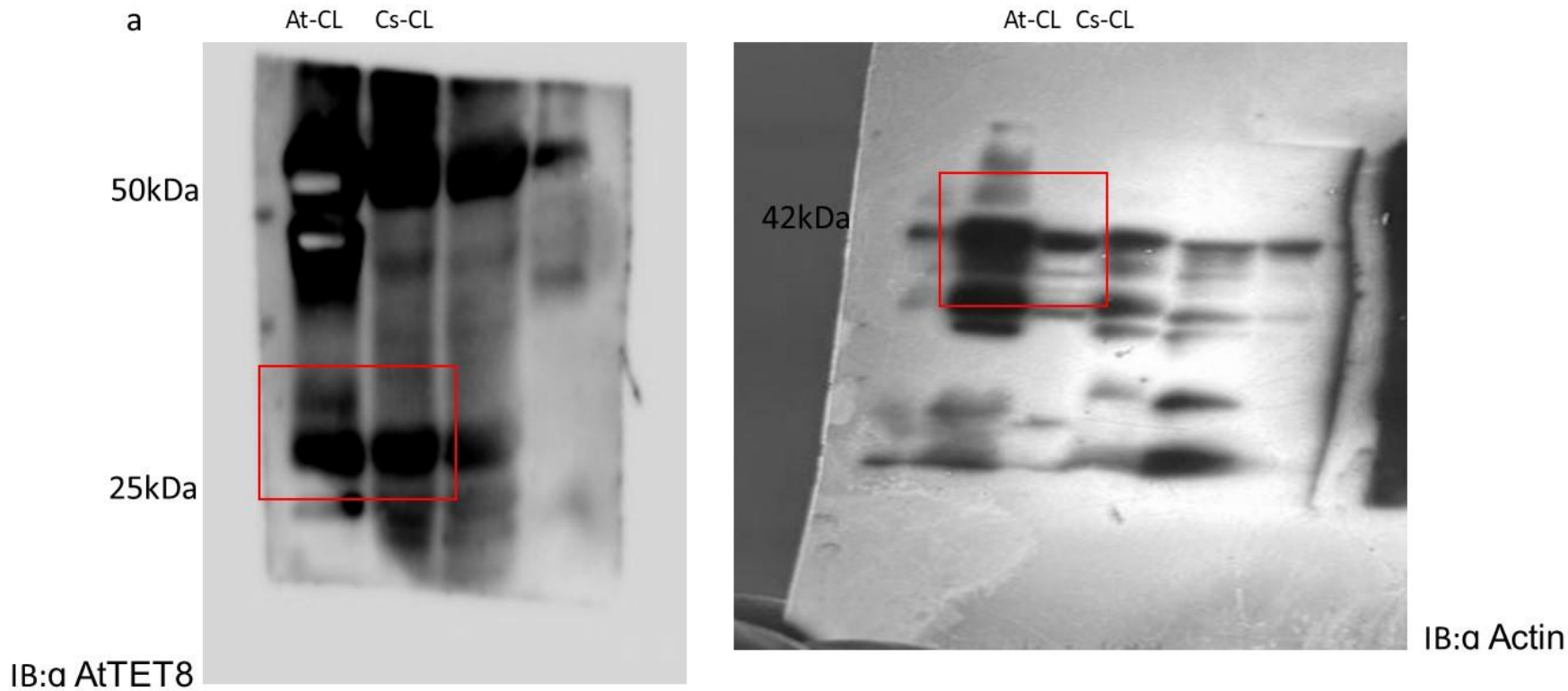


**Fig. 4 Characterization of CsTET8 and CsPP2 from EVs infected with ASSVd.**
(a) Western blot detection of TET8 in arabidopsis cell lysate (At-CL) cucumber cell lysates (Cs-CL) using Arabidopsis anti-AtTET8 antibody, revealing a band around 30 kDa, which corresponds to the size of TET8 in both Arabidopsis and cucumber CL (lower panel) western blot of the same extracts with anti-Actin antibody.

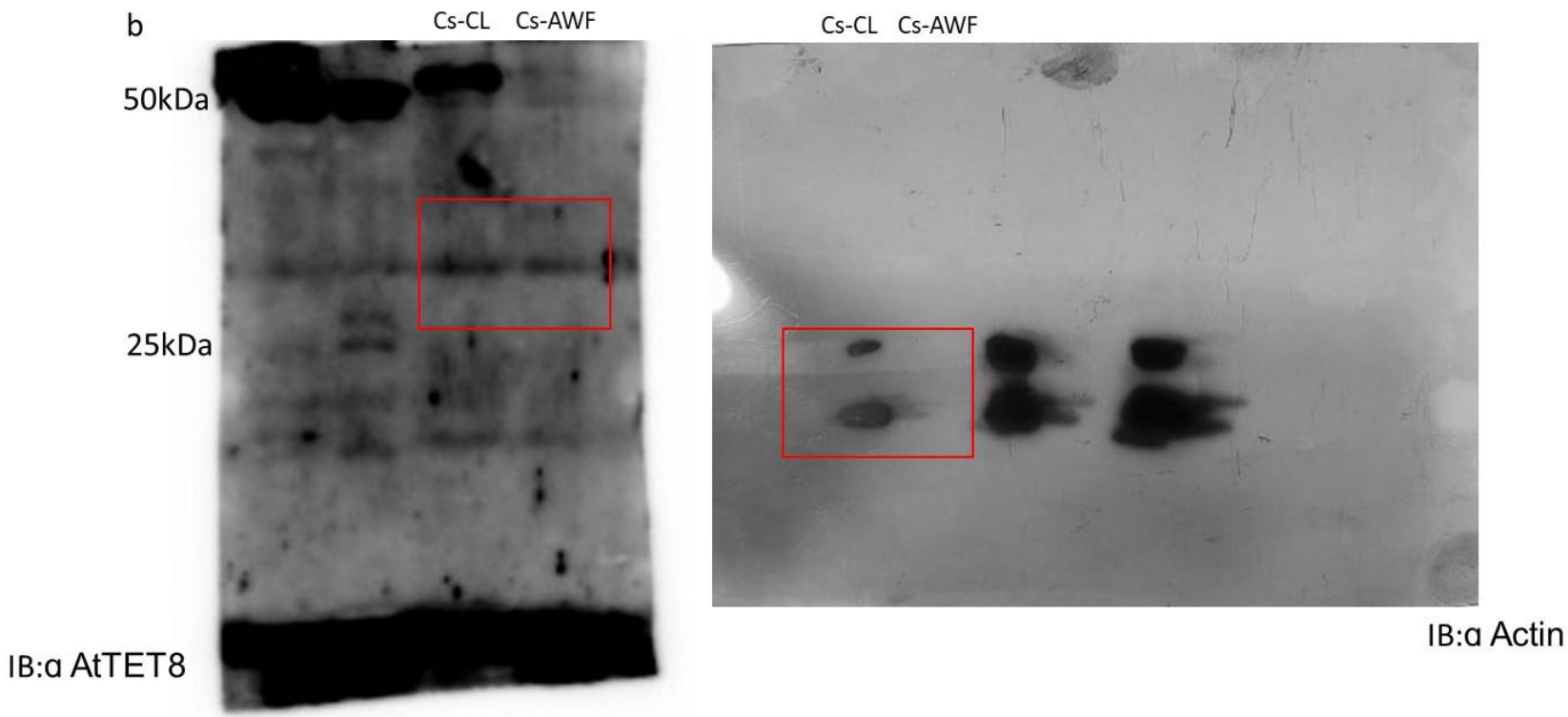


**Fig. 4**(b) Western blot of cucumber CL and AWF with anti-AtTET8 antibody. Western blot of the same extract with anti-actin antibody are used as loading controls.

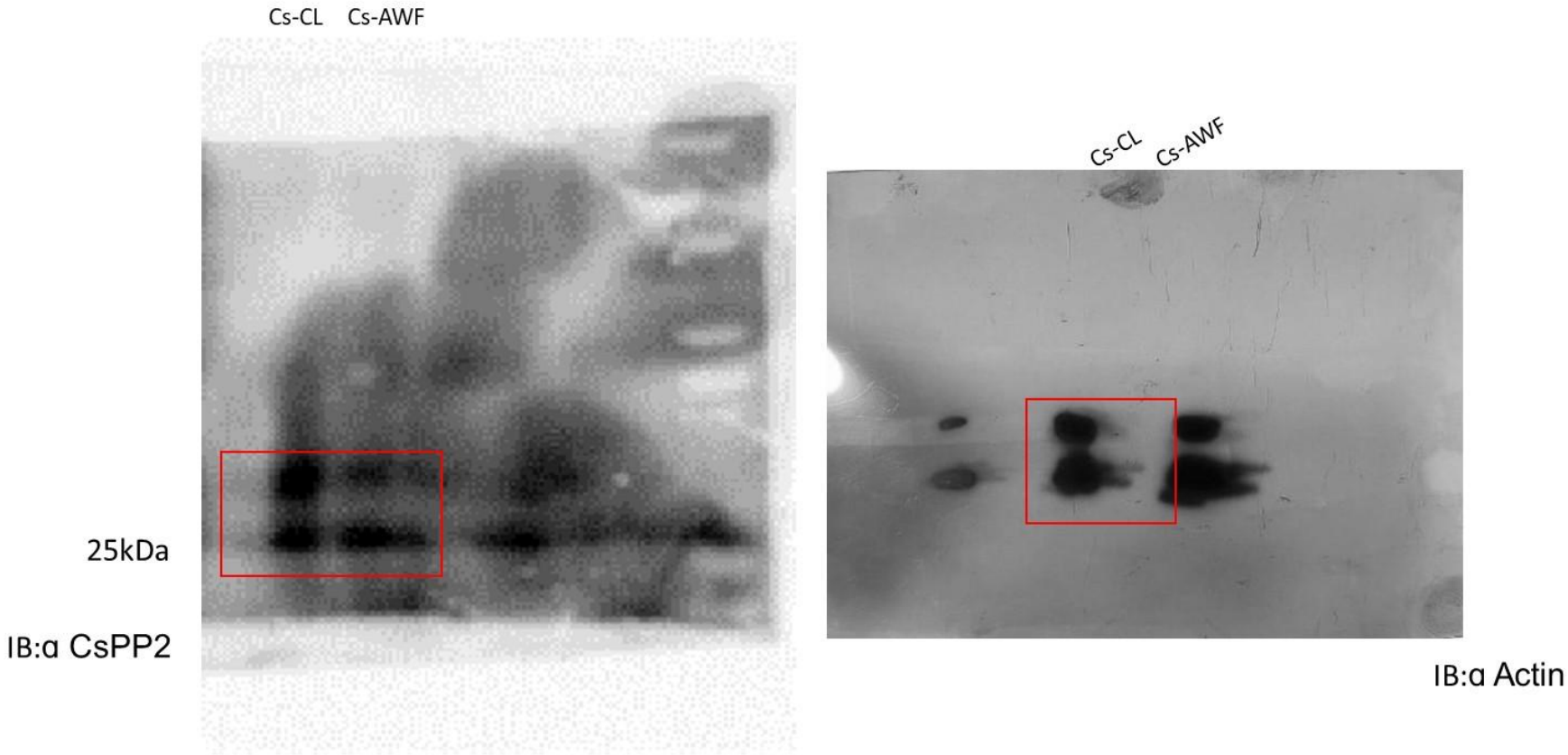


**Fig. 4**(b) Western blot of cucumber CL and AWF with anti-CsPP2 antibody. Western blot of the same extract with anti-actin antibody are used as loading controls.

c

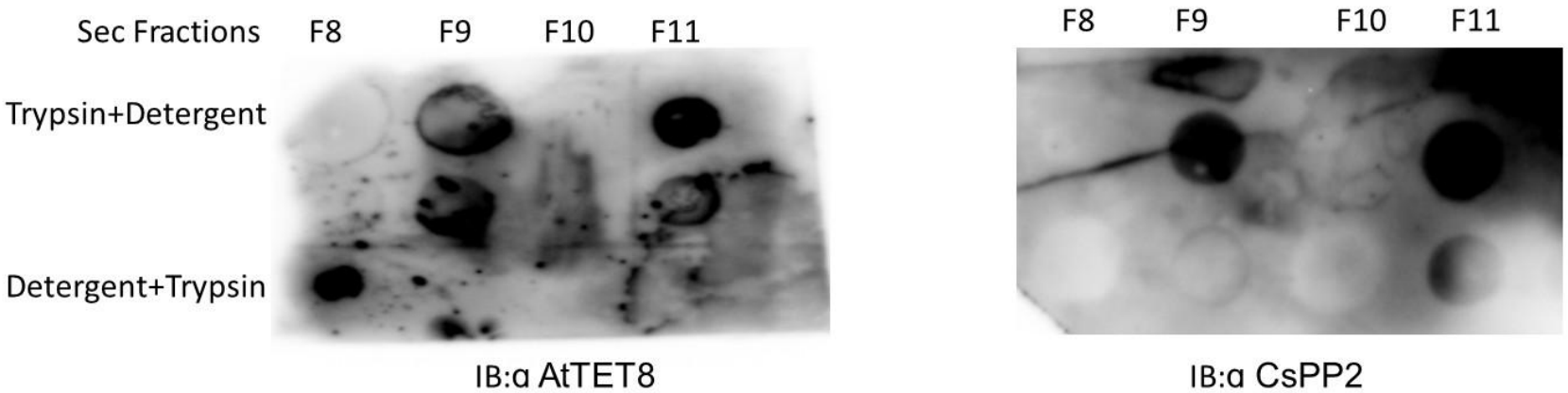


**Fig. 4** (c)Western blot analysis of EV fractions (8-11) isolated by SEC, using AtTET8 antibodies to detect CsTET8 and CsPP2 in fractions 9 and 11 (upper lane in upper and lower blot). The fractions were treated with trypsin to degrade the surface proteins of the EVs, followed by detergent-induced rupture before loading onto the membrane. The lower lane shows the degradation of CsTET8 and CsPP2 from inside the EVs when ruptured with detergent before trypsin digestion, suggesting both proteins are localized inside the EVs.

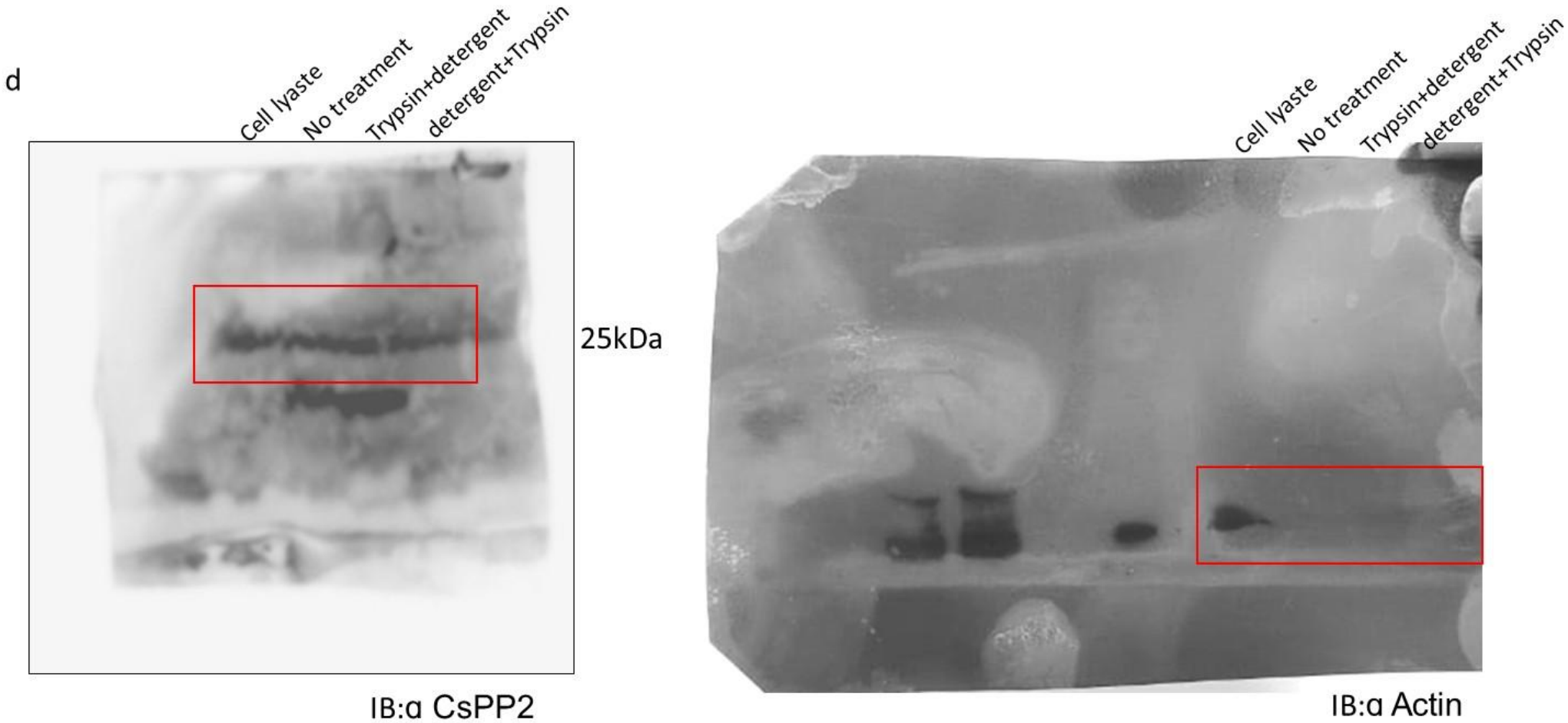


Fig. 4(d) Western blot analysis using anti-AtTET8 and anti-CsPP2 antibodies of pooled EV fractions (9 and 11) with different treatments—no treatment, trypsin followed by detergent, and detergent followed by trypsin—indicating that CsTET8 and CsPP2 are localized both inside and outside the EVs. Western blot of the same extract with anti-actin antibody are used as loading controls.

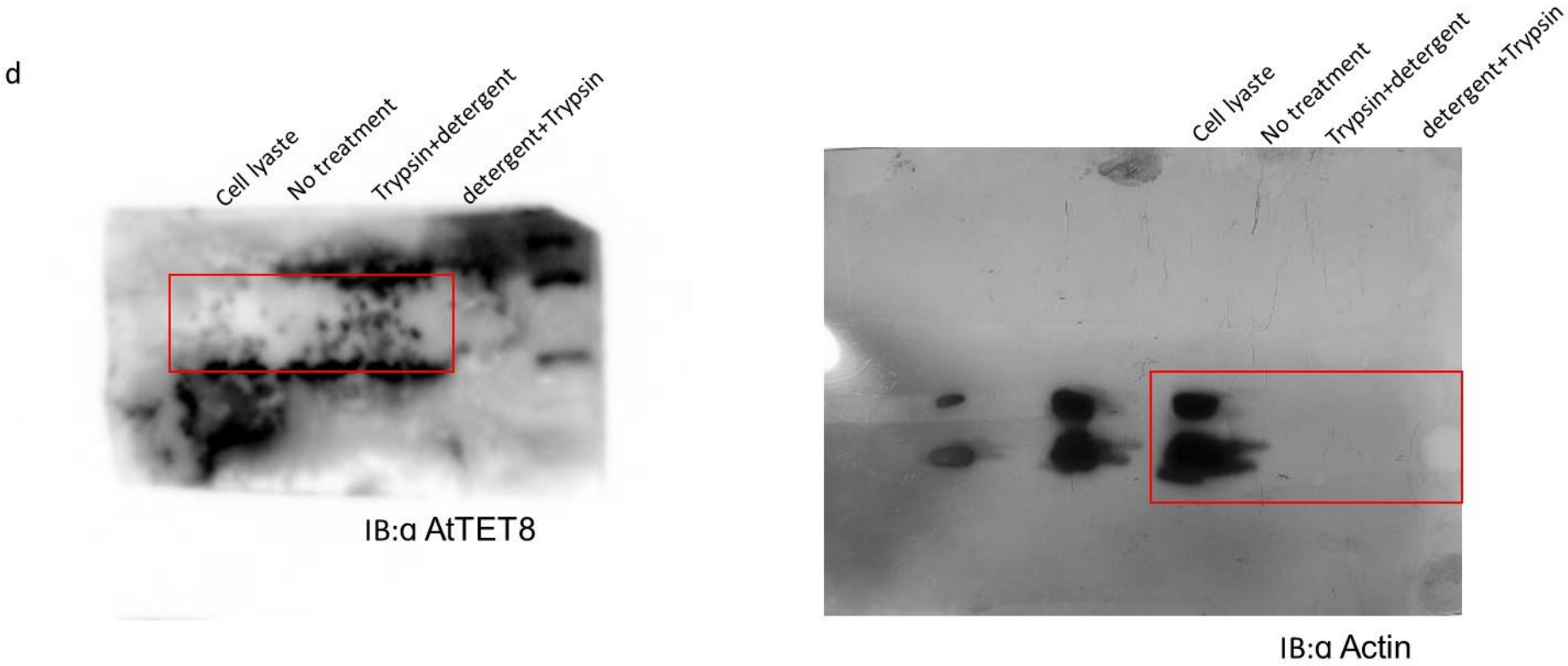


Fig. 4(d) Western blot analysis using anti-AtTET8 and anti-CsPP2 antibodies of pooled EV fractions (9 and 11) with different treatments—no treatment, trypsin followed by detergent, and detergent followed by trypsin—indicating that CsTET8 and CsPP2 are localized both inside and outside the EVs. Western blot of the same extract with anti-actin antibody are used as loading controls.

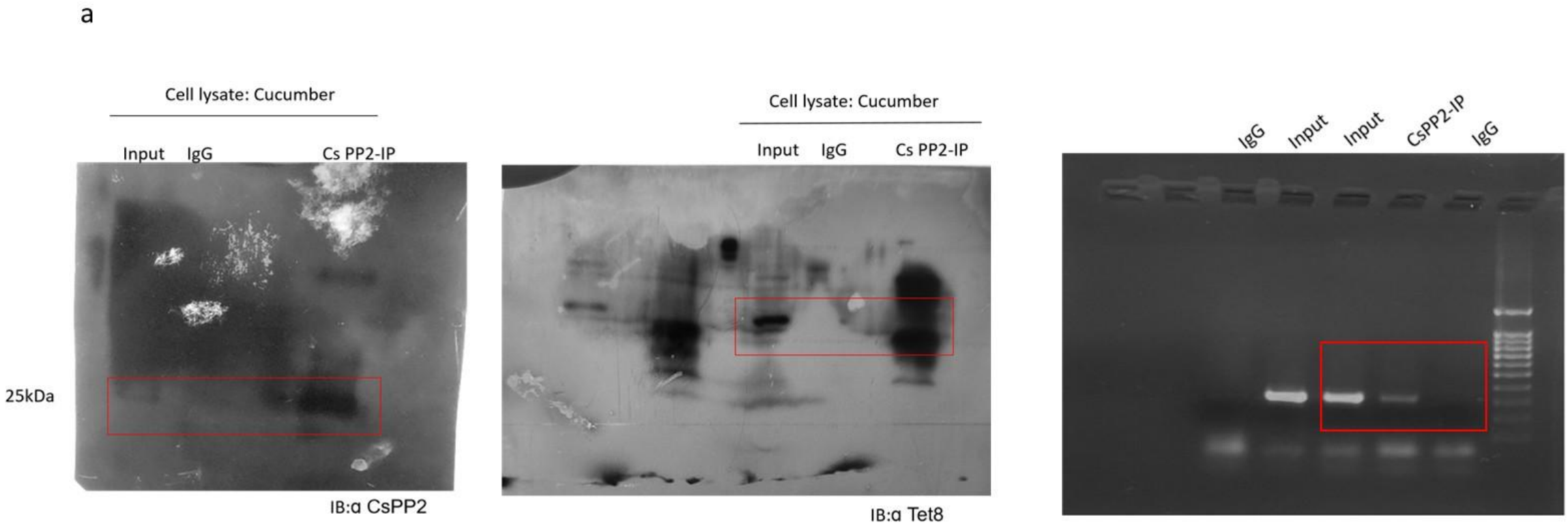


**Fig. 5 Interaction between CsPP2- CsTET8 and ASSVd in cytosol and extracellular space**

(a) Western blot analysis showing detection of CsPP2 in its immunoprecipitates from cell lysates (upper panel), along with co-detection of CsTET8 by western blot and ASSVd RNA by RT-PCR from the same sample.

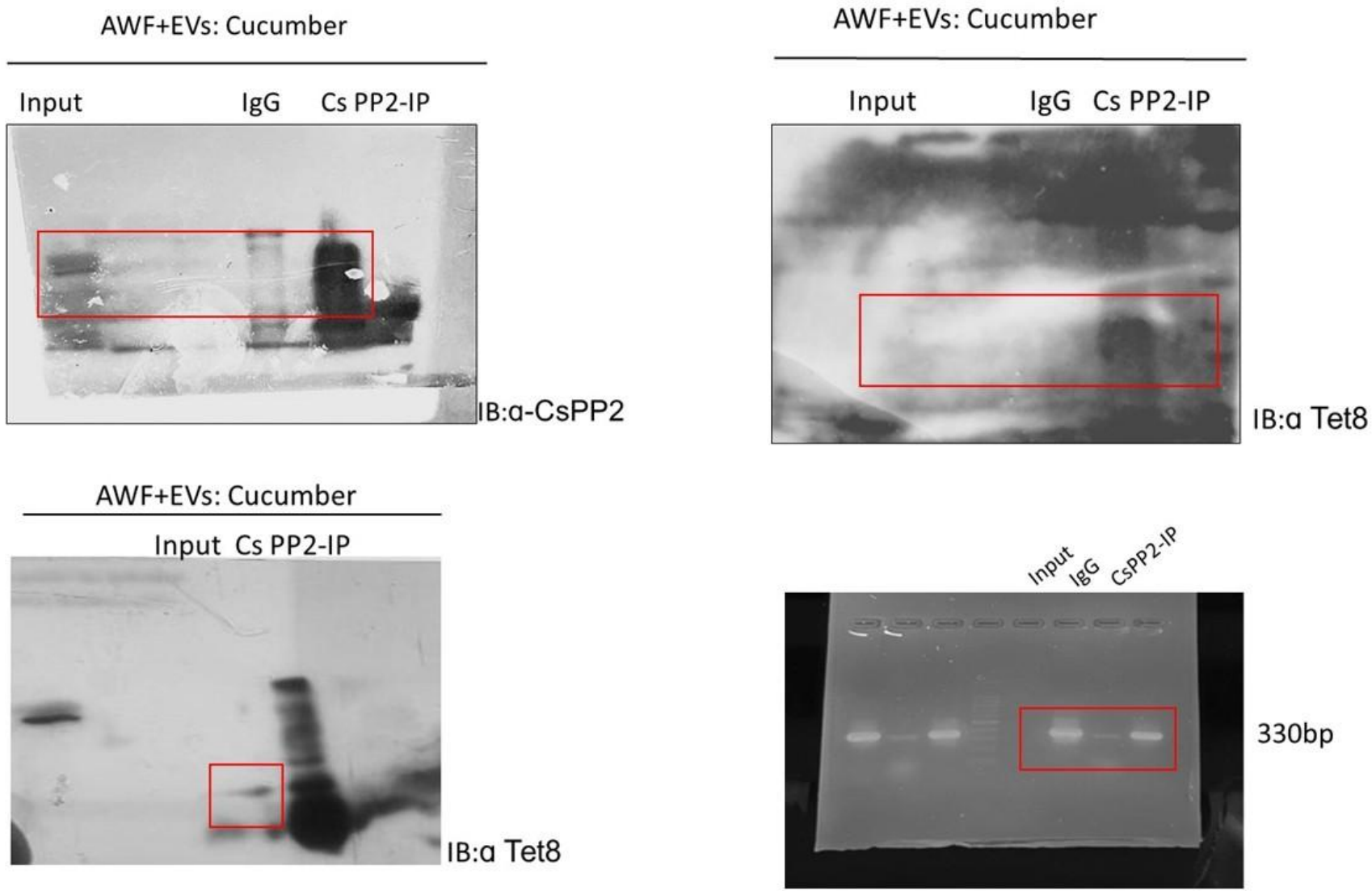


Fig. 5(b) Western blot showing CsPP2 immunoprecipitated from the apoplast + EVs fraction, with CsTET8 detected via western blot and ASSVd RNA via RT-PCR from the same sample.

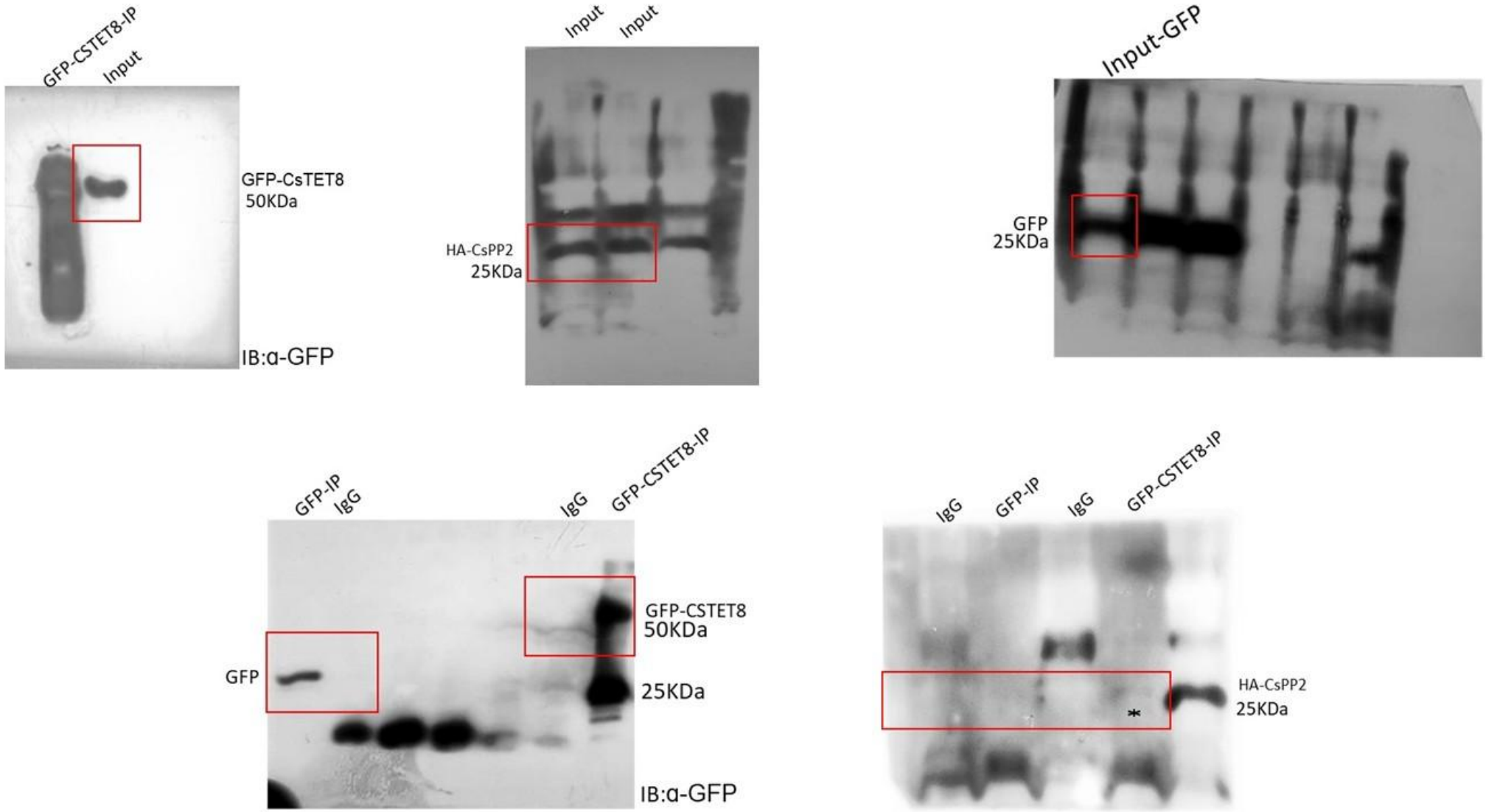


Fig.5 c Western blot of a co-immunoprecipitation assay demonstrating the interaction between GFP-TET8 and HA-PP2 when transiently expressed in *N. benthamiana*, using anti-GFP and anti-HA antibodies.

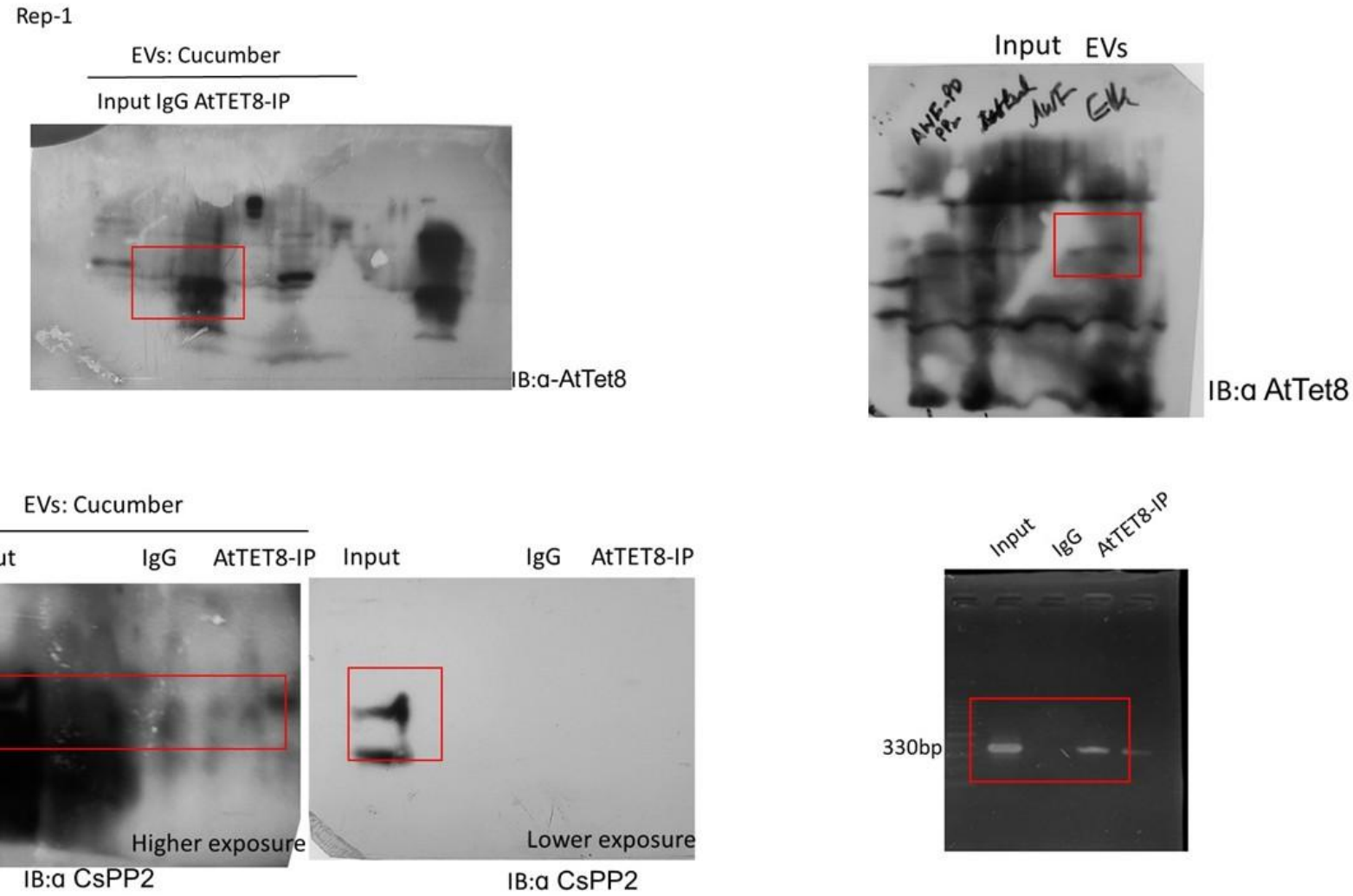


Fig. 5f Western blot showing immuno-enrichment of CsTET8-containing exosomes from the total EV pool, with co-detection of CsPP2 in the same sample. ASSVd RNA was also detected in the immuno-enriched exosomes using RT-PCR.

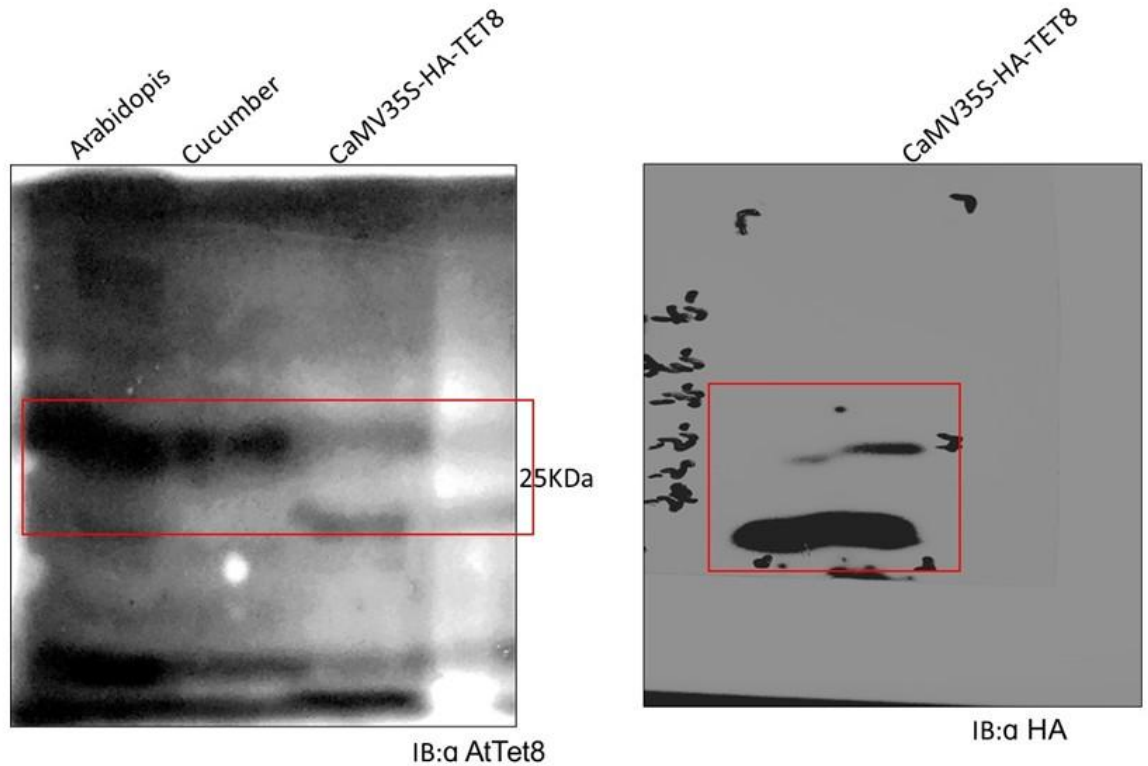


**Fig. S2d** western blot of *N. benthamiana* cell lysate (CL) showing transient expression of HA-CsTET8 and arabidopsis and cucumber cell lysate as control showing 30kDa band corresponding to the size of TET8 with anti-TET8 antibody and anti-HA antibody.

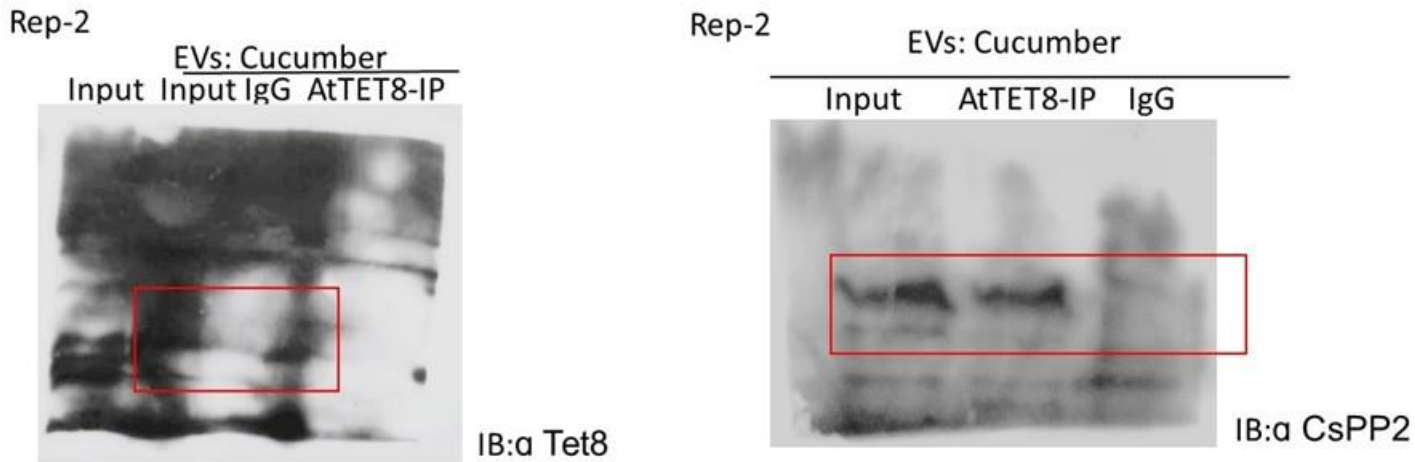


Western blot showing immuno-enrichment of CsTET8-containing exosomes from the total EV pool, with co-detection of CsPP2 in the same sample. ASSVd RNA was also detected in the immuno-enriched exosomes using RT-PCR.

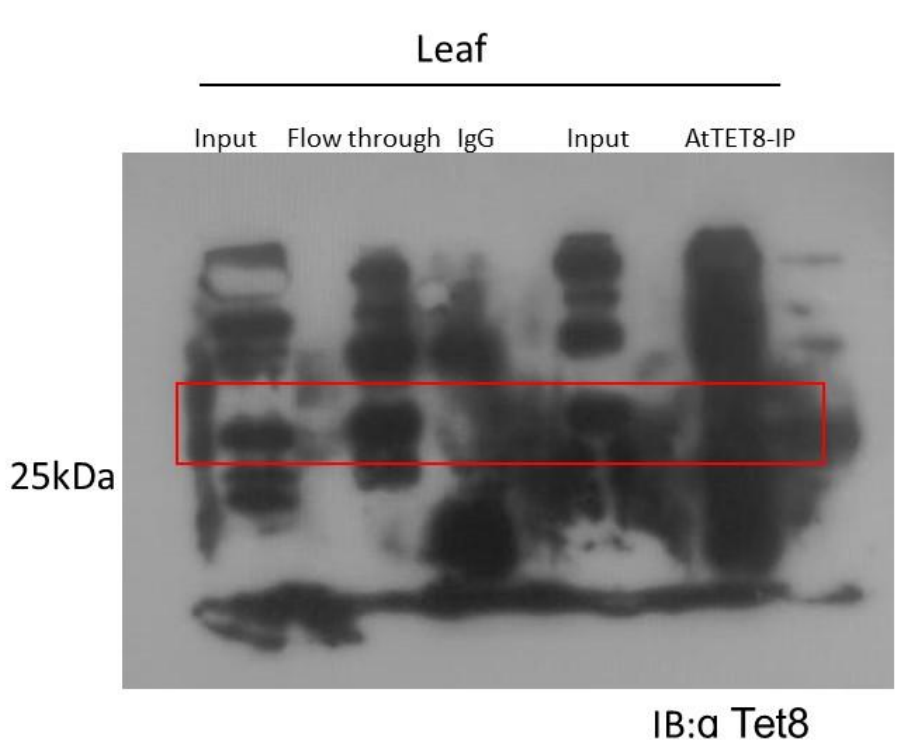


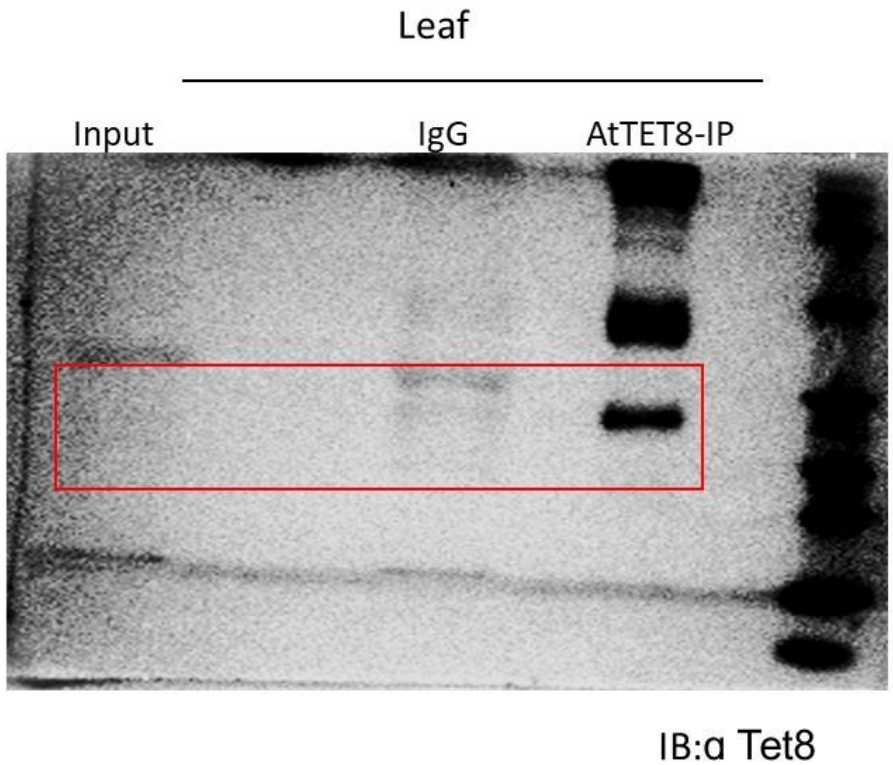


Western blot showing the At-TET8 IP using Cucumber cell lysate